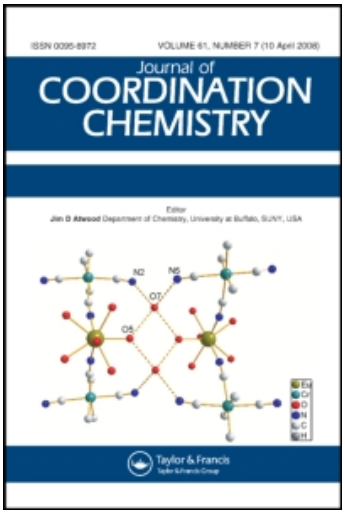

Journal of Coordination Chemistry
Publication details, including instructions for authors and subscription information:
http://www.informaworld.com/smpp/title~content=t713455674

An inorganic-organic compound with 1D honeycomb-like channels constructed from non-covalent linkage: synthesis and properties

Fan-Xia Meng[a]; Ya-Guang Chen[a]; Hai-Jun Pang[a]; Dong-Mei Shi[a]; Yu Sun[a]
[a] Key Laboratory of Polyoxometalates Science of Ministry of Education, College of Chemistry, Northeast Normal University, Changchun 130024, P.R. China

To cite this Article Meng, Fan-Xia , Chen, Ya-Guang , Pang, Hai-Jun , Shi, Dong-Mei and Sun, Yu(2008) 'An inorganic-organic compound with 1D honeycomb-like channels constructed from non-covalent linkage: synthesis and properties', Journal of Coordination Chemistry, 61: 10, 1513 — 1524
To link to this Article: DOI: 10.1080/00958970701598761
URL: http://dx.doi.org/10.1080/00958970701598761

Journal of Coordination Chemistry
Vol. 61, No. 10, 20 May 2008, 1513–1524

An inorganic-organic compound with 1D honeycomb-like channels constructed from non-covalent linkage: synthesis and properties

FAN-XIA MENG, YA-GUANG CHEN*,
HAI-JUN PANG, DONG-MEI SHI and YU SUN

Key Laboratory of Polyoxometalates Science of Ministry of Education,
College of Chemistry, Northeast Normal University, Changchun 130024, P.R. China

(*Received 8 February 2007; accepted 3 May 2007*)

An inorganic-organic hybrid compound $\{[Cu(phen)_3]_2PW_{11}VO_{40}\cdot 2H_2O$ (**1**) has been hydrothermally prepared and structurally characterized by elemental analyses, IR, CV, TG, magnetic susceptibility measurements and single crystal X-ray diffraction. Compound **1** crystallizes in the monoclinic space group $C2/c$ with $a=27.232(2)$ Å, $b=25.351(2)$ Å, $c=16.2748$ (4) Å, $\beta=105.20°$, $V=10842.3$ Å^3, $Z=4$, $R_1=0.0490$ and $wR_2=0.1362$. The structure of **1** exhibits a three-dimensional supramolecular network, formed by hydrogen-bonding and π–π stacking interactions. The three-dimensional network consists of one-dimensional honeycomb channels, which accommodate free water molecules. The size of the channel is 10.4×10.4 Å. Electrochemistry of **1** shows it undergoes three one-electron reversible redox processes. Variable-temperature magnetic measurements show typical antiferromagnetic interactions in the 2–300 K temperature range.

Keywords: Polyoxometalates; Inorganic-organic hybrid compound; Channel; Supramolecular framework

1. Introduction

Crystal engineering of porous inorganic-organic frameworks have structural diversity and potential applications in molecular adsorption, magnetism, ion exchange, heterogeneous catalysis, medicine and materials science [1]. Large numbers of macroporous crystalline materials constructed from metal-organic frameworks have been studied based on their gas storage, molecular sieve, shape-selective catalysis, and ion exchange properties [2, 3].

Polyoxometalates (POMs), as nanosized discrete metal-oxygen cluster anions with enormous structural variety and interesting properties [4], have been employed as inorganic building blocks for construction of crystalline solids in combination with appropriate metal-organic cations [5, 6]. Strategies directed toward design of open molecular networks have produced many porous frameworks with variable size cavities

*Corresponding author. Email: chenyg146@nenu.edu.cn

Journal of Coordination Chemistry
ISSN 0095-8972 print/ISSN 1029-0389 online © 2008 Taylor & Francis
DOI: 10.1080/00958970701598761

or channels [7–9]. Apart from covalent interactions, synthesized macro-porous materials also contain hydrogen-bonding and π–π stacking interactions in the supramolecular assembly.

Among polyoxometalate cluster anions, the first characterized and best known is the Keggin type [10]; recently, vanadium-containing tungstophosphate anions with Keggin structure $[PW_{12-n}V_n]^{(3+n)-}$ have been studied because vanadium-substituted Keggin anions are excellent catalysts in oxidation of organic compounds [11]. Vanadium-substituted polyoxotungstates based on Keggin frameworks were synthesized [12]. Porous supramolecular compounds containing Keggin frameworks have rarely been reported [13, 14]. Important goals in the preparation of porous structural supramolecular assemblies include establishing the connections between metal-organic and/or inorganic building blocks on the basis of interactions [15, 16] such as π–π stacking and hydrogen bonding interactions, and examining their properties such as magnetism, absorption-desorption, electro-chemistry, catalysis and so on. Because of POM's ability to undergo reversible multi-electron redox processes, they are very attractive in electrode modification and electrocatalytic research. Hybrid materials of POMs prepared by hydrothermal technique are usually insoluble in water and common organic solvents, important to applications in chemically bulk-modified carbon paste electrodes (CPE). Here we report the first macrocation-polyoxometalate supramolecular architecture $\{[Cu(phen)_3]_2PW_{11}VO_{40}\} \cdot 2H_2O$ with 1D honeycomb channels filled with free water; significant efforts will be devoted to the properties of **1**.

2. Experimental

2.1. *General procedures*

All reagents were of analytical grade and obtained from commercial sources without further purification. Distilled water was used in the reactions. Elemental analyses (C, H and N) were performed on a Perkin-Elmer 2400 CHN Elemental Analyzer. W, Cu and V were determined by a Leaman inductively coupled plasma (ICP) spectrometer. IR spectrum was recorded in the range 400–4000 cm^{-1} on an Alpha Centauri FT/IR spectrophotometer using KBr pellets. TG analysis was performed on a Perkin-Elmer TGA7 instrument in flowing N_2 with a heating rate of 10°C min^{-1}. Cyclic voltammograms were obtained with a CHI 660 electrochemical workstation at room temperature; platinum gauze was used as counter electrode and Ag/AgCl was used as reference electrode. A chemically bulk-modified CPE was used as working electrode. The magnetic properties have been performed on crystalline sample using a Quantum Design MPMS-5SQUID magnetometer in the range 2–300 K.

2.2. *Synthesis of* $\{[Cu(phen)_3]_2PW_{11}VO_{40}\} \cdot 2H_2O$

Compound **1** was prepared from reaction of $CuSO_4 \cdot 5H_2O$ (0.2335 g), phen (0.3378 g), $Na_3VO_4 \cdot 2H_2O$ (0.2983 g), Na_2WO_4 (1.0 g), 85% H_3PO_4 (5d) and 12 mL water. The starting mixture was adjusted to pH = 8.1 by the addition of 2 M NaOH and the mixture stirred for 30 min in air. The final solution was transferred to a 25 mL Teflon–lined autoclave and crystallized at 170°C for 6 days. Then the autoclave was cooled at

$10^{\circ}C\,h^{-1}$ to room temperature. The resulting yellow green block crystals were filtered off, washed with distilled water, and dried at ambient temperature. Good quality block crystals were sealed for structural determination and further characterization. Elemental analytical results of crystals are consistent with the stoichiometry of **1**. Anal. Calcd. for $\{[Cu(phen)_3]_2PW_{11}VO_{40}\}\cdot 2H_2O$ (%): C, 21.70; N, 4.22; W, 50.75; Cu, 3.19. Found: C, 21.82; N, 4.30; W, 50.62; Cu, 3.10.

2.3. *X-ray crystallography*

The structure of **1** was determined by single-crystal X-ray diffraction. A yellow green single crystal of **1** was carefully selected under a polarizing microscope and glued at the tip of a thin glass fiber with cyanoacrylate (superglue) adhesive. The data were collected on a Siemens Smart CCD diffractometer at 293 K using graphite-monochromated Mo$K\alpha$ radiation ($\lambda = 0.71073$ Å) and omega scans technique; an empirical absorption correction was applied. The structure was solved by direct methods and refined by full-matrix least-squares methods on F^2 using SHELXL 97 software [17]. All non-hydrogen atoms were refined anisotropically. Hydrogen atoms were added according to theoretical models and refined isotropically. The crystal data and structure refinement of **1** are summarized in table 1. Selected bond lengths and angles of **1** are listed in tables 2 and 3, respectively. Hydrogen bond lengths and angles are listed in table 4.

Table 1. Crystal data and structure refinement for **1**.

Empirical formula	$C_{72}H_{52}Cu_2N_{12}O_{42}PVW_{11}$
Formula weight	3988.60
Temperature (K)	293(2)
Wavelength (Å)	0.71073
Crystal system, space group	Monoclinic, $C2/c$
Unit cell dimensions (Å, °)	
a	27.232(2)
b	25.351(2)
c	16.2748(13)
α	90.00
β	105.200
γ	90.00
Volume (Å^3)	10842.3(15)
Z, Calculated density (Mg m^{-3})	4, 2.443
Absorption coefficient (mm^{-1})	12.176
$F(000)$	7256
Crystal size (mm^3)	$0.186 \times 0.171 \times 0.158$
Theta range for data collection (°)	1.55 to 26.00
Limiting indices	$-32 \le h \le 33$, $-31 \le k \le 30$, $-19 \le l \le 20$
Reflections collected/unique	29424/9930[$R(int) = 0.0542$]
Completeness to $\theta = 26.00$	93.1%
Refinement method	Full-matrix least-squares on F^2
Data/restraints/parameters	9930/7/661
Goodness-of-fit on F^2	0.934
Final R indices [$I > 2\sigma(I)$]	$R_1 = 0.0490$, $wR_2 = 0.1362$
Extinction coefficient	0.000038(7)
Largest diff. peak and hole (e Å^{-3})	1.956 and −1.550

Table 2. Selected bond lengths [Å] for **1**.

Cu(1)–N(2)	2.073(15)	Cu(1)–N(5)	2.141(9)
Cu(1)–N(3)	2.099(11)	Cu(1)–N(4)	2.147(11)
Cu(1)–N(1)	2.135(11)	Cu(1)–N(6)	2.155(10)
W(1)–O(16)	1.621(10)	W(2)–O(6)	1.690(8)
W(1)–O(13)	1.839(11)	W(2)–O(5)	1.864(10)
W(1)–O(15)	1.843(10)	W(2)–O(8)	1.891(10)
W(1)–O(14)	1.866(9)	W(2)–O(17)	1.899(10)
W(1)–O(17)	1.871(10)	W(2)–O(7)	1.907(11)
W(1)–O(2)	2.377(14)	W(2)–O(1)	2.443(13)
W(1)–O(3)	2.457(16)	W(4)–O(12)	1.687(10)
W(3)–O(10)	1.655(9)	W(4)–O(18)	1.862(10)
W(3)–O(14)#1	1.884(9)	W(4)–O(13)	1.886(11)
W(3)–O(19)#1	1.904(11)	W(4)–O(5)	1.916(9)
W(3)–O(8)	1.905(9)	W(4)–O(11)	1.923(12)
W(3)–O(9)	1.910(10)	W(4)–O(4)	2.415(17)
W(3)–O(1)	2.430(14)	W(6)–O(20)	1.676(10)
W(5)–O(22)	1.663(9)	W(6)–O(19)	1.857(11)
W(5)–O(9)	1.849(9)	W(6)–O(21)	1.859(11)
W(5)–O(11)	1.876(11)	W(6)–O(18)	1.860(10)
W(5)–O(21)	1.894(9)	W(6)–O(7)#1	1.871(12)
W(5)–O(15)#1	1.909(10)	W(6)–O(4)	2.496(15)
W(5)–O(4)	2.402(15)	W(6)–O(1)#1	2.509(16)
P(1)–O(3)	1.407(16)	P(1)–O(1)	1.521(14)
P(1)–O(2)	1.483(13)	P(1)–O(4)	1.547(17)

Symmetry transformations used to generate equivalent atoms: 1 $-x+1/2$, $-y+1/2$, $-z+1$.

Table 3. Selected bond angles (°) for **1**.

N(2)–Cu(1)–N(3)	93.4(5)	N(3)–Cu(1)–N(5)	97.1(4)
N(2)–Cu(1)–N(1)	78.5(5)	N(1)–Cu(1)–N(5)	94.3(5)
N(3)–Cu(1)–N(1)	94.0(4)	N(2)–Cu(1)–N(4)	98.1(5)
N(2)–Cu(1)–N(6)	91.7(4)	N(3)–Cu(1)–N(4)	77.9(4)
N(1)–Cu(1)–N(6)	92.4(4)	N(5)–Cu(1)–N(4)	90.5(4)
N(5)–Cu(1)–N(6)	78.5(4)	N(4)–Cu(1)–N(6)	95.9(4)
O(16)–W(1)–O(13)	103.2(6)	O(17)–W(1)–O(2)	66.0(5)
O(16)–W(1)–O(15)	101.8(6)	O(16)–W(1)–O(3)	162.6(6)
O(13)–W(1)–O(15)	155.0(5)	O(13)–W(1)–O(3)	88.7(5)
O(16)–W(1)–O(14)	102.2(6)	O(15)–W(1)–O(3)	66.8(5)
O(13)–W(1)–O(14)	86.5(4)	O(14)–W(1)–O(3)	65.5(5)
O(15)–W(1)–O(14)	87.7(4)	O(17)–W(1)–O(3)	91.0(5)
O(16)–W(1)–O(17)	102.2(6)	O(2)–W(1)–O(3)	35.5(5)
O(13)–W(1)–O(17)	86.6(4)	O(13)–W(1)–O(2)	63.6(5)
O(15)–W(1)–O(17)	88.8(5)	O(15)–W(1)–O(2)	92.1(5)
O(14)–W(1)–O(17)	155.6(5)	O(14)–W(1)–O(2)	90.0(4)
O(16)–W(1)–O(2)	161.8(6)	O(3)–P(1)–O(4)	109.0(9)
O(3)–P(1)–O(2)	61.4(8)	O(2)–P(1)–O(4)	72.4(8)
O(3)–P(1)–O(1)	108.5(8)	O(1)–P(1)–O(4)	105.0(8)
O(2)–P(1)–O(1)	72.7(8)		

Table 4. Hydrogen bond lengths (Å) and angles (°) for **1**.

D–H···A	d(D–H)	d(H···A)	d(D···A)	∠(DHA)
C10–H10···O22	0.930	2.296	3.166	155.28
C21–H21···O10	0.930	2.588	3.216	125.34
C28–H28···O11	0.930	2.604	3.130	116.33
C28–H28···O5	0.930	2.596	3.212	124.10
C23–H23···O1W	0.930	2.683	3.340	128.26
O1W···O6	0.930		2.951	

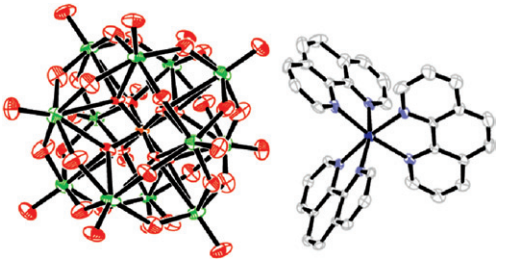

Figure 1. Ortep drawing of **1**. The hydrogen atoms are omitted for clarity.

2.4. *Preparation of {[Cu(phen)$_3$]$_2$PW$_{11}$VO$_{40}$ · 2H$_2$O}-CPE (1-CPE)*

The **1**-CPE was fabricated as follows: 96 mg graphite powder and 8 mg compound **1** were mixed and ground together by agate mortar and pestle to achieve an even, dry mixture. To the mixture, 0.05 mL paraffin oil was added and stirred with a glass rod. Then the homogenized mixture was used to pack a 3 mm inner diameter glass tube, and the surface was wiped with glass paper. Electrical contact was established with copper rod through the back of the electrode.

3. Results and discussion

3.1. *Crystal structure of (1)*

Single crystal X-ray structure analysis revealed that **1** consists of one discrete anion $[PW_{11}VO_{40}]^{4-}$, two coordination cations $[Cu(phen)_3]^{2+}$ and two water molecules (see figure 1). The water molecule OW2 is disordered over two positions with 50% occupancy. The anion is a classic Keggin anion (general formula $[PM_{12}O_{40}]^{n-}$), central heteroatom P exhibits $\{PO_4\}$ tetrahedral geometry, and coordinated M atoms exhibit $\{MO_6\}$ octahedral configuration; each three $\{MO_6\}$ octahedra constitute a tri-metal cluster $\{M_3O_{13}\}$ in edge-sharing mode; four such corner-sharing clusters $\{M_3O_{13}\}$ are arrayed around the central $\{XO_4\}$ tetrahedron. The M–O bonds can be divided into three groups, M–O_t bonds fall in the range 1.621(10)–1.690(8), M–$O_{b/c}$ bonds fall in the range 1.839(11)–1.923(12) and M–O_a bonds are in the range 2.402(15)–2.509(16) Å. The mean M–O_t and M–$O_{b/c}$ distances are shorter than reported in the literature [18], and the mean value of the M–O_a distance is somewhat longer [18], indicating that the MO_6 octahedra of the Keggin anion are slightly distorted. In **1**, there exist two $\{PO_4\}$ tetrahedral groups with each Oa site half-occupied, forming an almost regular cube, namely cubic eight-coordinate for P; the P–Oa distances are in the range 1.407(16)–1.547(17) Å. The V atom substitutes for a W atom from its parent anion $[PW_{12}O_{40}]^{3-}$, but the V does not lie in a fixed position and distributes in twelve sites variously; twelve M positions are crystallographically disordered with different occupancies for W and V.

In the $[Cu(phen)_3]^{2+}$ unit, Cu is defined by six N atoms of three phen ligands in a distorted $\{CuN_6\}$ octahedron with Cu–N bond distances ranging from 2.073(15) to 2.155(10) Å and bond angles of N–Cu–N varying from 77.9°(4) to 98.1°(5), indicating that the copper(II) centers are a '4 + 2' distorted octahedron.

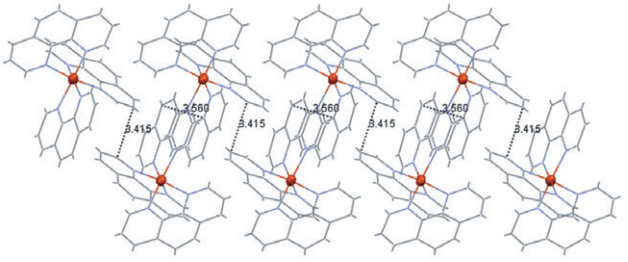

Figure 2. Copper coordination cation columns formed by π-π interactions of phen molecules parallel to the *b*-axis.

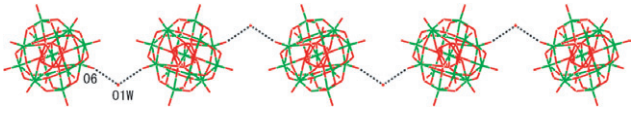

Figure 3. The 1D twist chain-like diagram of polyoxoanions of **1** viewed from the *c* axis.

There are significant $\pi\cdots\pi$ stacking interactions of phen rings with interplane separations of 3.415–3.560 Å (as shown in figure 2). Copper coordination cations form columns by head-to-head and face-to-face aromatic ring $\pi\cdots\pi$ interactions. Besides $\pi\cdots\pi$ interactions of aromatic rings, the whole crystal structure of **1** is strengthened by hydrogen bonding. The crystalline water molecules (O1W) form hydrogen bonds with surface oxygen atoms of the Keggin anion; the inorganic anion clusters extend its linkage into a 1D infinite twist chain *via* a short O(6) and O1W distance (2.951 Å), as shown in figure 3. Chains of inorganic anions and copper coordination cation columns array crossly, further joined by hydrogen-bonding to form a 3D supramolecular framework.

The crystal structure is a three-dimensional supramolecular framework with one-dimensional 'honeycomb-like' channels along [001] figure 4 with dimensions of approximately $10.4 \times 10.4\,\text{Å}^2$. The weak linkage between the hydrogen atoms of phen ring and surface oxygen atoms of Keggin units are hydrogen-bonding interactions, with distances of C(phen) – H$\cdots$O(POM)(11) in the range 3.130–3.340 Å table 4. The whole crystal is stabilized by $\pi\cdots\pi$ interactions of aromatic rings and hydrogen-bonding interactions; hydrogen bonds are usually important in synthesis of supramolecular architectures [19, 20] and play an important role in the stabilization of **1**.

The assignments of oxidation state for Cu, W and V are consistent with their coordination geometries and confirmed by valence sum calculations [21]. Bond valence analysis shows that all W atoms are in the +6 oxidation state, V atom is in the +5 oxidation state and copper is in the +2 oxidation state.

3.2. *Characterization*

3.2.1. IR spectrum. The IR spectrum of **1** is shown in figure S1. There are four characteristic asymmetric vibrations from the polyanion $[PVW_{11}O_{40}]^{4-}$ at 956, 881 and 792 cm^{-1}, assigned to stretching vibrations of ν_{as}(W–O_t), ν_{as} (W–O_b–W) and

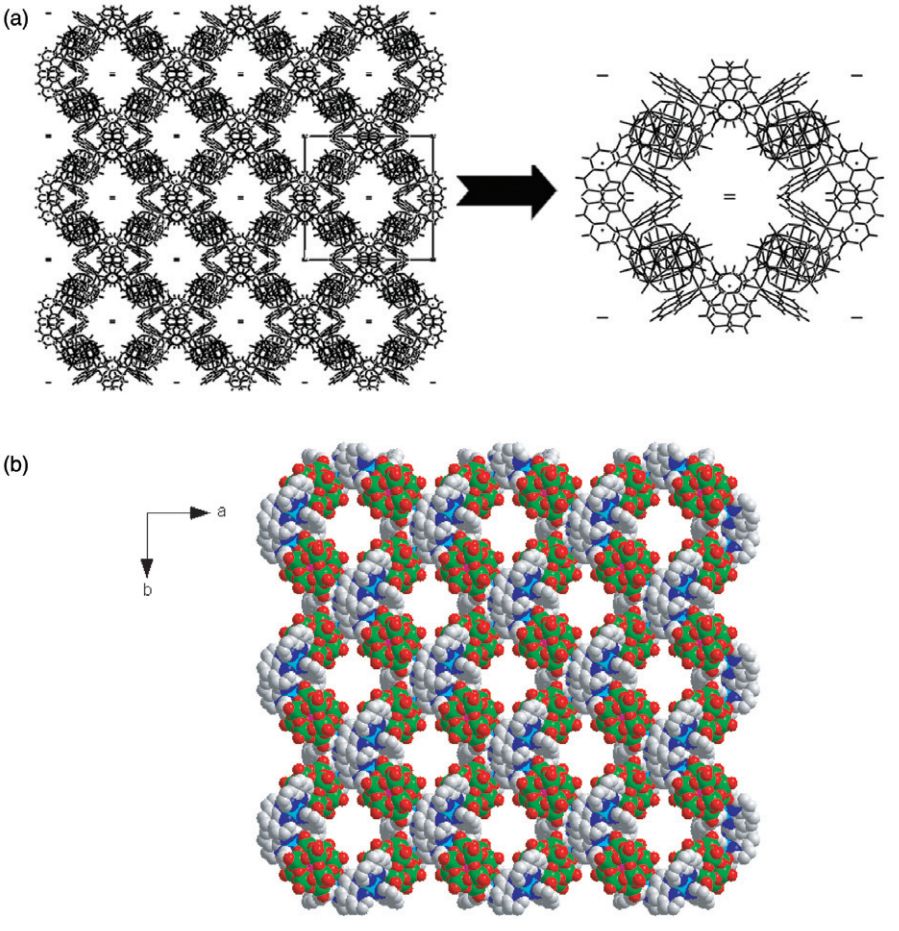

Figure 4. (a) Packing diagram of the three-dimensional supramolecular framework of **1**, viewed along the *c* axis, highlighting the honeycomb-like channels; (b) Space filling diagram of 3D supramolecular framework of **1** (color code: W/V, green; P, yellow; O, red; Cu, sky blue; N, blue; C, gray). Disordered water molecules are omitted for clarity.

ν_{as}(W–O_c–W), respectively. Bands at 1076 and 1058 cm^{-1} can be assigned to P–O stretching vibrations. Compared with a typical value at 1067 cm^{-1} for the Keggin anion [22, 23], the P–O stretch of the mono-substituted Keggin tungstophosphate anion splits into two bands because of the lower symmetry. Features at 1624, 1520 and 1435 cm^{-1} are attributed to stretching vibrations of C–N and C=N bonds of phen. Features at 1215 and 1136 cm^{-1} are ascribed to ring stretching of 1,10′-phenanthroline [24]. The broad band at 3427 cm^{-1} is characteristic of H_2O.

3.2.2. TG analysis. The TG curve (figure S2) of **1** showed three weight loss stages, giving a total loss of 28.17% in the range 44–851°C, which agrees with the calculated value of 28.04%. The weight loss (1.22%) of the first step (44–177°C) corresponds to

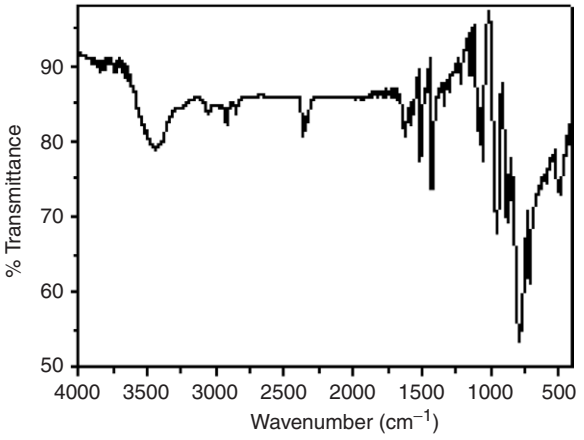

Scheme 1. The IR spectrum of compound **1**.

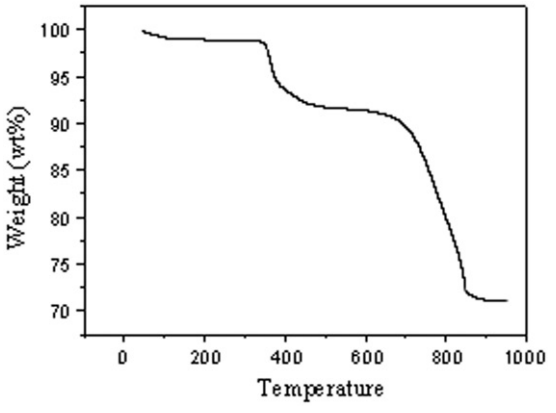

Scheme 2. The TG curve of compound **1**.

release of all free water. The weight loss (26.95%) of the second and third step (332–851°C) arise from decomposition of phen (calcd 27.11%).

3.2.3. Cyclic voltammetry of 1–CPE. Figure S3 shows the cyclic voltammetric behavior of **1**-CPE in 0.2 M Na_2SO_4+H_2SO_4 (pH = 0.04) solution at different scan rates. In the potential range from −950 to 1200 mV, three reversible one-electron redox peaks appear and the mean peak potentials $E_{1/2} = (Ecp + Eap)/2$ are +401, −110 and −535 mV, respectively. The two negative redox peaks correspond to reduction of the W^{VI} centers [25–27] and the positive redox peak is ascribed to $V^{V} \rightarrow V^{IV}$ [28]. With the scan rate varying from 20 to 200 $mV \cdot s^{-1}$, the peak potentials change gradually, cathodic peak potentials shift toward the negative and corresponding anodic peak potentials to the positive. The peak-to-peak separation between corresponding cathodic and anodic peaks increases with the scan rate increasing, common for CPE with POM [29]. The encapsulation of **1** into CPE may slow penetration of protons from solution into the particles, thus decreasing the electron exchange rate between **1** and electrode.

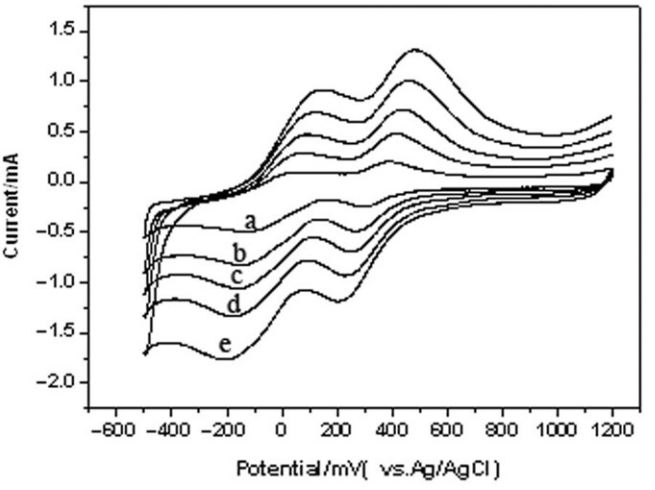

Scheme 3. Cyclic voltammograms of the **1**-CPE in the 0.2 M $Na_2SO_4 + H_2SO_4 + H_2SO_4$ (pH = 0.04) solution at different scan rates: (a) 20, (b) 50, (c) 100, (d) 150 and (e) 200 $mV \cdot S^{-1}$.

POMs are very sensitive to pH and therefore changes in the pH are expected to affect the electrochemical properties of POMs. Figure S4 shows the electrochemical behavior of **1**-CPE in a 0.2 M Na_2SO_4+H_2SO_4 aqueous solution with different pH values at a scan rate of 50 $mV \cdot s^{-1}$. The pH of the supporting electrolyte solution has slight effect on the electrochemical behavior of **1**-CPE, with increasing pH, three reversible redox peaks gradually shift to negative and the peak currents decrease.

3.2.4. Magnetic susceptibility. The magnetic properties have been performed on a crystalline sample using a Quantum Design MPMS-5SQUID magnetometer in the range 2–300 K. The variable-temperature magnetic behavior at fixed field strength of 1000 Oe for **1** is shown in figure 5 in the form of $\chi_m T$ vs. T and $1/\chi_m$ *vs.* T curves. This behavior of the $\chi_m T$ curve indicates that antiferromagnetic interactions exist in **1**. At 300 K, the effective magnetic moment (μ_{eff}) determined from $\mu_{eff} = 2.828(\chi_m T)^{1/2}$ is 3.15 μ_B, which is higher than that expected for two uncoupled Cu(II) ions (2.45 μ_B, 0.75 emu K mol^{-1}, considering g = 2), suggesting contributions of orbit magnetic moment. When decreasing the temperature, the $\chi_m T$ of **1** decreases gradually from 1.24 at 300 K to 1.12 cm^3 K mol^{-1} at 2 K, typical for paramagnetic systems with antiferromagnetic interactions. The thermal variation of the molar susceptibility follows the Curie–Weiss law [$\chi_m = C/(T\text{-}\theta)$] in the range 2–300 K. The value of the Curie constant C and the Weiss constant θ are 1.24 emu K mol^{-1} and −4.1 K, respectively. These results indicate antiferromagnetic interactions in **1**.

4. Conclusion

In summary, we have prepared and structurally characterized an organic–inorganic hybrid compound based on Keggin polyoxoanions and copper coordination complexes.

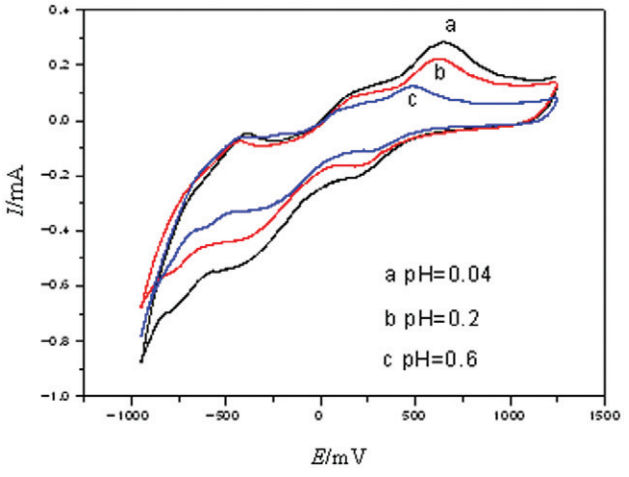

Scheme 4. The cyclic voltammograms for the **1**-CPE in 0.2 M $Na_2SO_4 + H_2SO_4$ solutions with different pH values: (a) 0.04; (b) 0.2; (c) 1.6. Scan rate: $50\,mV \cdot s^{-1}$.

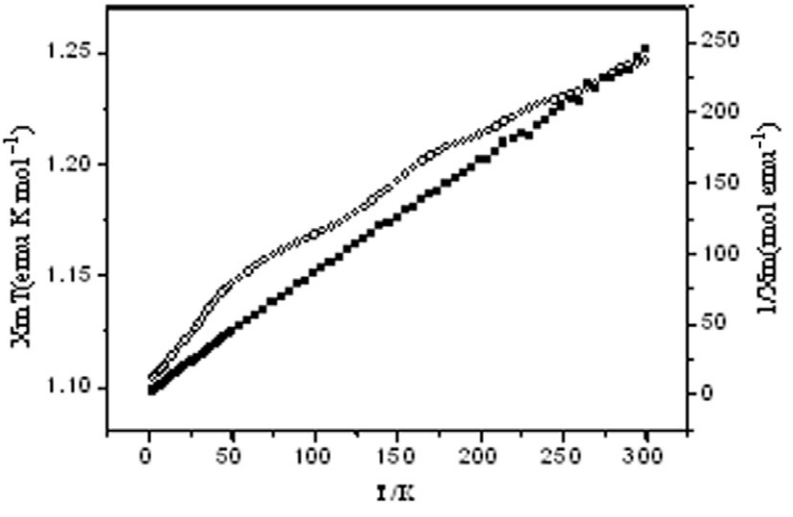

Figure 5. Temperature dependence of $\chi_m T$ and $1/\chi_m$ (in inset) for **1**.

It represents the first example of porous frameworks containing vanadium-substituted Keggin heteropolytungstate. In **1**, copper coordination cations form columns *via* face-to-face and head-to-head π–π interactions. Free water molecules link polyoxoanions into 1D infinite twist chains. The anion chains of inorganic cluster and cation columns are further joined by hydrogen-bonding to form a 3D supramolecular framework with one-dimensional 'honeycomb-like' channels. The cyclic voltammetric behavior of **1**-CPE reveals three reversible one-electron redox peaks; the scan rate and pH of solution have an effect on the peak potentials. We tried to replace copper with other transition metals, but no crystals were found. Further research may focus on replacement of phen with other organo-nitrogen ligands to prepare neutral porous compounds and explore their valuable properties.

Supplementary material

Crystallographic data (excluding structure factors) for the structure(s) reported in the article have been deposited with the Cambridge Crystallographic Data Centre as Supplementary publication No. CCDC: 603592. Copies of the data can be obtained free of charge on application to CCDC, 12 Union Road, Cambridge CB2 IEZ, UK (Fax: +44-1223-336-033; Email: deposit@ccdc.cam.ac.uk or http://www.ccdc.cam.ac.uk).

Acknowledgements

This work was supported by the Analysis and Testing Foundation of Northeast Normal University.

References

[1] (a) M.E. Davis. *Nature*, **417**, 813 (1992); (b) A. Corma, F. Rey, S. Valencia, J.L. Jorda, J.A. Rius. *Nat. Mater.*, **2**, 493 (2003); (c) S.M. Kuznicki, V.A. Bell, H.W. Hillhouse, R.M. Jacubinas, C.M. Braunbarth, B.H. Toby, M. Tsapatsis. *Nature*, **412**, 720 (2001).
[2] T.J. Barton, L.M. Bull, W.G. Klemeperer, D.A. Loy, B. McEnaney, M. Misono, P.A. Monson, G. Pez, G.W. Scherer, J.C. Vartuli, O.M. Yaghi. *Chem. Mater.*, **11**, 2633 (1999).
[3] K. Yamamoto, Y. Sakata, Y. Nohara, Y. Takahashi, T. Tatsumi. *Science*, **300**, 470 (2003).
[4] (a) M.T. Pope. Heteropoly and Isopoly Oxometalates, Springer, Berlin (1983); (b) M.T. Pope, A. Müler. *Angew. Chem.*, **103**, 56 (1991); (c) C.L. Hill, C.M. Prosser-McCartha. *Coord. Chem. Rev.*, **143**, 407 (1995).
[5] (a) M. Hölscher, U. Englert, B. Zibrowius, W.F. Hölderich. *Angew. Chem., Int. Ed. Engl.*, **33**, 2491 (1994); (b) D. Hagrman, P.J. Hagrman, J. Zubieta. *Angew. Chem. Int. Ed.*, **38**, 3165 (1999); (c) W. Schmitt, E. Baissa, A. Mandel, C.E. Anson, A.K. Powell. *Angew. Chem. Int. Ed.*, **40**, 3577 (2001); (d) Y. Ishii, Y. Takenaka, K. Konishi. *Angew. Chem. Int. Ed.*, **43**, 2702 (2004); (e) S.S. Mal, U. Kortz. *Angew. Chem. Int. Ed.*, **44**, 3777 (2005).
[6] (a) Y. Hayashi, F. Müller, Y. Lin, S.M. Miller, O.P. Anderson, R.G. Finke. *J. Am. Chem. Soc.*, **119**, 11401 (1997); (b) M.I. Khan, E. Yohannes, D. Powell. *Inorg. Chem.*, **38**, 212 (1999); (c) J.H. Son, H. Choi, Y.U. Kwon. *J. Am. Chem. Soc.*, **122**, 7432 (2000); (d) M.V. Vasylyev, R. Neumann. *J. Am. Chem. Soc.*, **126**, 884 (2004).
[7] X.L. Wang, Y.Q. Guo, Y.G. Li, E.B. Wang, C.W. Hu, N.H. Hu. *Inorg. Chem.*, **42**, 4135 (2003).
[8] H.Y. An, D.X. Xiao, E.B. Wang, Y.G. Li, X.L. Wang, Y. Lu. *Eur. J. Inorg. Chem.*, **44**, 854 (2005).
[9] Y.G. Li, N. Hao, E.B. Wang, M. Yuan, C.W. Hu, N.H. Hu, H.Q. Jia. *Inorg. Chem.*, **42**, 2729 (2003).
[10] (a) J.F. Keggin. *Nature*, **131**, 908 (1933); (b) J.F. Keggin. *R. Proc. Soc. London Ser. A*, **144**, 75 (1934).
[11] R. Neumann, M. Lissel. *J. Org. Chem.*, **54**, 4607 (1989).
[12] (a) C.M. Flynn, M.T. Pope. *Inorg. Chem.*, **10**, 2745 (1971); (b) C.M. Flynn, Jr., M.T. Pope. *Inorg. Chem.*, **11**, 1950 (1972).
[13] R. Kawamoto, S. Uchida, N. Mizuno. *J. Am. Chem. Soc.*, **127**, 10560 (2005).
[14] S. Uchida, R. Kawamoto, N. Mizuno. *Inorg. Chem.*, **45**, 5136 (2006).
[15] (a) J.-M. Lehn. *Science*, **295**, 2400 (2002); (b) G.R. Desiraju. *Angew. Chem., Int. Ed. Engl.*, **34**, 2311 (1995); (c) H. Kumagai, M. Arishima, S. Kitagawa, K. Ymada, S. Kawata, S. Kaizaki. *Inorg. Chem.*, **41**, 1989 (2002).
[16] (a) B.J. Holliday, C.A. Mirkin. *Angew. Chem. Int. Ed.*, **40**, 2022 (2001); (b) S. Kawata, S.R. Breeze, S. Wang, J.E. Greedan, N.P. Raju. *Chem. Commun.*, 717 (1997); (c) J. Dai, M. Yamamoto, T. Kuroda-Sowa, M. Maekawa, Y. Suenaga, M. Munakata. *Inorg. Chem.*, **36**, 2688 (1997); (d) Y.B. Dong, M.D. Smith, R.C. Layland, H.C. Loye. *Inorg. Chem.*, **38**, 5027 (1999).
[17] G.M. Sheldrick. *SHELXTL 97, Program for Crystal Structure Refinement*, University of Göttingen (1997).
[18] E. Burkholder, V. Golub, C.J. O'Connor, J. Zubieta. *Inorg. Chem. Commun.*, **3**, 363 (2004).
[19] M.J. Krische, J.M. Lehn. *Struct. Bonding*, **96**, 3 (2000).

[20] (a) M. Yuan, Y.G. Li, E.B. Wang, Y. Lu, C.W. Hu, N.H. Hu, H.Q. Jia. *J. Chem. Soc., Dalton Trans.*, 2916 (2002); (b) Z.B. Han, E.B. Wang, G.Y. Luan, Y.G. Li, H. Zhang, Y.B. Duan, C.W. Hu, N.H. Hu. *J. Mater. Chem.*, **12**, 1169 (2002).
[21] I.D. Brown, D. Altermatt. *Acta Crystallogr.*, **B41**, 244 (1985).
[22] C. Rocchiccioli-Deltcheff, M. Fournier, R. Franck, R. Thouvenot. *Inorg. Chem.*, **22**, 207 (1983).
[23] R. Massart, R. Contant, F.J.M. Ruchart, J.P. Ciabrini, M. Fournier. *Inorg. Chem.*, **16**, 2916 (1977).
[24] Y.G. Li, E.B. Wang, S.T. Wang, Y.B. Duan, C.W. Hu, N.H. Hu, H.Q. Jia. *J. Mol. Struct.*, **611**, 185 (2002).
[25] M. Sadakane, E. Steckhan. *Chem. Rev.*, **98**, 219 (1998).
[26] B.S. Bassil, U. Kortz, A.S. Tigan, J.M. Clemente-Juan, B. Keita, P. de Oliveira, L. Nadjo. *Inorg. Chem.*, **44**, 9360 (2005).
[27] (a) B. Botar, Y.V. Geletii, P. Kögerler, D.G. Musaev, K. Morokuma, I.A. Weinstock, C.L. Hill. *Dalton Trans.*, 2017 (2005); (b) L. Ruhlmann, J. Canny, R. Contant, R. Thouvenot. *Inorg. Chem.*, **41**, 3811 (2002); (c) D. Jabbour, B. Keita, I.M. Mbomekalle, L. Nadjo, U. Kortz. *Eur. J. Inorg. Chem.*, 2036 (2004).
[28] D.E. Clinton, D.A. Tryk, I.T. Bae, F.L. Urbach, M.R. Antonio, D.A. Scherson. *J. Phys. Chem.*, **100**, 18511 (1996).
[29] X.L. Wang, Z.H. Kang, E.B. Wang, C.W. Hu. *J. Electroanal. Chem.*, **523**, 142 (2002).